ResearchGate

See discussions, stats, and author profiles for this publication at: https://www.researchgate.net/publication/259091519

A theoretical contribution to the characterization of the low-lying electronic states of BeBr including spin-orbit effects

ARTICLE *in* JOURNAL OF MOLECULAR SPECTROSCOPY · JANUARY 2014

Impact Factor: 1.48 · DOI: 10.1016/j.jms.2013.10.007

CITATIONS
5

READS
77

2 AUTHORS:

José Carlos Barreto de Lima
Federal Institute of Education, Science and …
4 PUBLICATIONS **18** CITATIONS

SEE PROFILE

Fernando Ornellas
University of São Paulo
129 PUBLICATIONS **1,187** CITATIONS

SEE PROFILE

Available from: José Carlos Barreto de Lima
Retrieved on: 25 January 2016

Journal of Molecular Spectroscopy 295 (2014) 1–6

Contents lists available at ScienceDirect

Journal of Molecular Spectroscopy

journal homepage: www.elsevier.com/locate/jms

A theoretical contribution to the characterization of the low-lying electronic states of BeBr including spin–orbit effects

José Carlos Barreto de Lima, Fernando R. Ornellas *

Universidade de São Paulo, Instituto de Química, Departamento de Química Fundamental, Av. Prof. Lineu Prestes, 748, São Paulo, SP 05508-000, Brazil

ARTICLE INFO

Article history:
Received 9 October 2013
In revised form 26 October 2013
Available online 5 November 2013

Keywords:
Beryllium monobromide
Potential energy curves
Spectroscopic parameters
Transition moments
Transition probabilities
Radiative lifetimes

ABSTRACT

Electronic states of BeBr correlating with the first two dissociation channels are investigated at a high level of electronic structure theory (CASSCF/MRCI) along with quintuple-zeta quality basis sets. Very reliable potential energy curves are constructed and regions of both avoided and curve crossings that greatly resemble the ones for BeCl are identified. For both the ground state (X $^2\Sigma^+$) and the first excited one (A $^2\Pi$), this study corroborates the present still limited experimental knowledge about this system and significantly extends its spectroscopic characterization. For the three doublets in the interval between 30 000 and 40 000 cm^{-1}, the inclusion of spin–orbit effects neatly accounts for the interactions between the relativistic states. For the A – X band system, transition moments were evaluated and transition probabilities, as expressed by the Einstein emission coefficients, computed; radiative lifetimes completed the characterization of the A state. The C $^2\Sigma^+$ state was found to have two minima in the $\Lambda + S$ representation, the first one with just one vibrational level; this shallow potential then disappears when perturbations by the B $^2\Pi$ and the a $^4\Sigma^+$ states are taken into account.

© 2013 Elsevier Inc. All rights reserved.

1. Introduction

Of the three species in the series of beryllium monohalides, BeF, BeCl, and BeBr, the beryllium monobromide molecule is the one least known experimentally. In a brief note by Reddy and Rao [1], the first report on a BeBr investigation dates back to 1967, with the observation of a bluish color emission when a mixture of bromine and argon was passed over warm beryllium metal powder and attributed to transitions in BeBr. Later expanded in an article [2], the authors describe three sequences of bands degraded to longer wavelengths in the region of 3660–3920 Å. In analogy with the already known spectra of BeF and BeCl, they attributed the bands to transitions of the A $^2\Pi$ – X $^2\Sigma^+$ system, and reported vibrational quantum formulae representing the Q_1, R_1, and R_2 heads. A reinvestigation of BeBr by Reddy et al. under high dispersion, including isotope shift analysis, provided next a more accurate set of spectroscopic constants for the X and A states [3]. A rotational analysis study on the 0–0 band of the A $^2\Pi$ – X $^2\Sigma^+$ system, performed by Carleer et al. [4], resulting in the determination of the internuclear distance R_0 and the rotational constant B_0 for both X $^2\Sigma^+$ and A $^2\Pi$ states, the spin–orbit coupling constant for the A $^2\Pi$ state, and the transition energy (T_{00}) was the only other reference to an experimental investigation on BeBr, to the best of our knowledge. Concerning the experimental difficulties of carrying out a rotational analysis of bands of BeBr at the time, Carleer et al. noted that besides the need of a very high resolution spectrograph, this system in particular has very similar vibrational constants for both the X $^2\Sigma^+$ and A $^2\Pi$ states, thus leading to a strongly overlapping sequence of bands. In addition, the nearly equal abundance of two of the bromine isotopes doubled the number of branches to be analyzed. An estimate of the dissociation energy of BeBr (D_0 = 71 kcal mol^{-1}) based on a correlation of thermochemical properties across the entire alkaline earth halide series was reported by Kleinschmidt and Hildenbrand [5]; this value differs significantly from the empirical determination of Reddy et al., 91.31 kcal mol^{-1} [6]. Theoretically, not a single study on the electronic states of BeBr has been found in the literature, with the exception of an early attempt at estimating theoretically the intensities of A $^2\Pi$ – X $^2\Sigma^+$ transitions by Kuz'menko and Chumak [7] through the calculation of Franck–Condon factors using a Morse potential energy function.

In contrast to BeBr, beryllium monochloride (BeCl) has been more thoroughly investigated in the literature both experimentally and theoretically, as recently reported by Lima and Ornellas [8]. Although the electronic states of BeBr are expected to show close similarities to those of BeCl, a reliable theoretical investigation of its electronic structure and spectroscopic parameters is certainly warranted. In this work, our major focus is the characterization of the electronic states of BeBr in a manner similar to that already done for BeCl [8]. Potential energy curves for a manifold of low-lying electronic states, including spin–orbit interactions, are

* Corresponding author.
E-mail address: frornell@usp.br (F.R. Ornellas).

0022-2852/$ - see front matter © 2013 Elsevier Inc. All rights reserved.
http://dx.doi.org/10.1016/j.jms.2013.10.007

constructed that can account in a reliable way for the observed and the as yet not observed electronic spectra of this species, especially the characterization of regions of avoided crossings, and crossings that can lead to predissociation. Besides the determination of spectroscopic parameters, we also evaluated the transition moment function, and radiative transition probabilities for A – X transitions, as estimated by the Einstein emission coefficients $A_{v'v''}$; radiative lifetimes of vibrationally excited states of the A $^2\Pi$ state were also estimated. By quantitatively accounting for the properties of this system, the present study is expected to provide an accurate global picture of a manifold of electronic states of BeBr, and thus reliable data to guide further experimental spectroscopic investigations.

2. Methodology

In analogy with our previous study on the BeCl system, the focus of this investigation is the set of states of BeBr correlating with the lowest-lying dissociation channel, Be (^1S_g) + Br (^2P_u), namely, $^2\Sigma^+$ and $^2\Pi$, and those leading to the second dissociation channel, Be (^3P_u) + Br (^2P_u), associated with the atomic states $^{2,4}\Sigma^+$ (2), $^{2,4}\Sigma^-$, $^{2,4}\Pi$ (2), and $^{2,4}\Delta$, according to the Wigner–Witmer rules [9].

In order to account simultaneously for bond breaking of the ground and excited states, a two step process involving first a state-averaged complete active space self-consistent (SA-CASSCF) [10,11] calculation followed by another one of the multireference configuration interaction (MRCI) type was the basic theoretical method used to describe the electronic structure of this system. The MRCI calculation used the internally contracted approach as implemented in the Molpro-2009 suite of programs [12–14]. In this latter step, we have correlated the 1*s* electrons of the Be atom but not included the 1*s* orbital in the active space of the CASSCF calculation. In the SA-CASSCF calculation all possible distributions of nine electrons in nine orbitals comprising the active space (5,2,2,0) were allowed. Besides the valence orbitals, the active space includes one extra orbital of A_1 symmetry to increase the flexibility of the reference space and thus to improve the quality of the wavefunction in regions of avoided crossings identified in test calculations. This notation implies that the orbitals transform according to the irreducible representations (A_1,B_1,B_2,A_2) of the C_{2v} point group, since most computer programs use Abelian subgroups to classify the orbitals and electronic states. The correspondence between the representations in the $C_{\infty v}$ and C_{2v} point groups is: $A_1(\Sigma^+, \Delta)$, $B_1(\Pi_x)$, $B_2(\Pi_y)$, $A_2(\Sigma^-, \Delta)$. In the SA-CASSCF step we mixed five states of A_1 symmetry, four states of B_1 and B_2 symmetries, and two states of A_2 symmetry.

For this choice of active space, the dimension of the reference space resulted in 2308 (1408) configuration state functions (CSF) for the doublet (quartet) states of A_1 symmetry, 2200 (1440) for those of B_1 and B_2 symmetries, and 2112 (1472) for the ones of A_2 symmetry. In the MRCI step, the configuration space ranged from about 4.0 to 7.5 million CSF for the doublets, and 2.0–3.1 million for the quartets. The molecular orbitals used to construct the N-particle basis are in fact state-averaged natural orbitals obtained by the diagonalization of an average density matrix for each one of the spin symmetries. In the expansion of the molecular orbitals, we used the set cc-pwCV5Z for beryllium [15] and aug-cc-pV5Z bromine [16], briefly V5Z.

Total energies were evaluated at about 60 internuclear distances and used to generate a numerical potential for the nuclear motion by the interpolation of about 2000 distances. This potential was next used in the solution of the Schrödinger radial equation by the Numerov–Cooley method as implemented in the Intensity Program [17], thus allowing the determination of vibrational energies, vibrationally averaged properties, and transition probabilities. The total energies used to generate the potential for the nuclear motion were corrected by an estimate of the contribution of the missing higher excitations needed to reach the full configuration interaction limit known as the Davidson correction (+Q) [18,19]. In the determination of spectroscopic parameters, we have used standard fitting procedures as described in previous studies [20–23].

Einstein spontaneous emission coefficients, $A_{v',v''}$ (in s^{-1}), were evaluated by the expression given below for the case of rotationless potentials

$$A_{v',v''} = 7.2356 \times 10^{-6} |D_{v',v''}|^2 \nu^3_{v',v''} \frac{(2-\delta_{0,\Lambda'+\Lambda''})}{(2-\delta_{0,\Lambda'})}$$

and used to estimate radiative transition probabilities. Here, $\nu_{v',v''}$ is the transition energy, and $(2-\delta_{0,\Lambda'+\Lambda''})/(2-\delta_{0,\Lambda'})$ is the degeneracy factor [24,25]. The multiplication constant is the appropriate factor to express the probabilities in s^{-1}, when the transition moment is given in units of eÅ, and the energy in cm^{-1}. In this expression, $D_{v',v''}$ stands for the transition dipole moment operator matrix element evaluated as

$$D_{v',v''} = \langle v'|D(R)|v''\rangle$$

where $|v'\rangle$ and $|v''\rangle$ represent the upper and lower state vibrational wavefunctions, and $D(R)$ is the transition dipole moment function evaluated over the whole range of internuclear distances at the MRCI level of theory. As usual, radiative lifetimes were evaluated as the inverse of the total Einstein $A_{v'}$ coefficients, which implies summing the transition probabilities to all lower vibrational states in all lower electronic states. In the evaluation of transition probabilities, we considered the recommendations given by Whiting et al. [26]. In this respect, the concise report by Larsson [27] summarizes for the reader the various conversion factors between the transition moment and other dynamical variables.

Finally, to estimate spin–orbit effects on the energies we have used the interacting states method with the spin–orbit matrix elements evaluated with the one- and two-electrons Breit–Pauli operators [28] at the MRCI level of theory along a quadruple-zeta quality basis set; this calculation also correlated the 1*s* electrons of beryllium. As implemented on the Molpro-2009 package, the spin–orbit eigenstates were obtained by diagonalizing the matrix representation of the $H_{el} + H_{SO}$ operator, constructed by the replacement of the diagonal elements of $H_{el} + H_{SO}$ matrix by the corresponding MRCI + Q/V5Z values.

3. Results and discussion

3.1. Potential energy curves, vibrational energies, and spectroscopic parameters

The profiles of the potential energy curves (PEC) of the doublet and quartet Λ + S states here investigated are depicted in Fig. 1, and for the bound ones the associated sets of spectroscopic parameters are summarized in Table 1. For the ground (X $^2\Sigma^+$) and the first excited (A $^2\Pi$) states for which very accurate experimental data on the internuclear distance R_0 have been determined by Carleer et al. [4], 3.6911 a_0 (1.9532 Å) and 3.7351 (1.9765 Å), respectively, this study predicts equilibrium distances (R_e) of 3.694 a_0 (1.955 Å) and 3.731 a_0 (1.975 Å) in very good agreement with the experimental results. As to the excitation energy (T_{00}), we have obtained 26 654 cm^{-1} (see discussion below), a value also in good accord with that reported by Carleer et al., 26437.6 cm^{-1} [4]. Concerning the vibrational constants (ω_e, $\omega_e x_e$) for the species $Be^{79}Br$, our estimates are (715.9, 3.592 cm^{-1}) for the ground state X $^2\Sigma^+$, and (700.0, 3.492 cm^{-1}) for the state A $^2\Pi$. Comparison of these results with the available experimental data for the Q_1 band head reported by Reddy et al. [3], (715.06, 4.30) and (702.29, 3.98), also shows a very good agreement. As another check of the

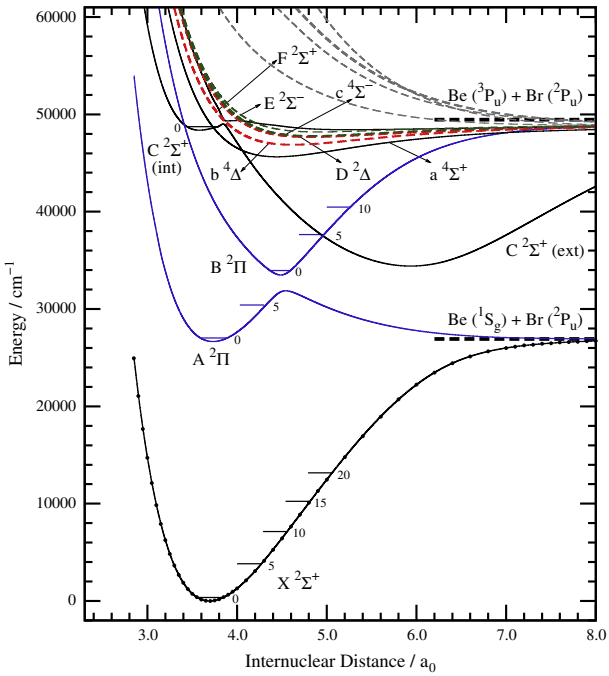

Fig. 1. Potential energy curves of the lowest-lying Λ + S doublet and quartet states of the molecule BeBr.

expected accuracy of the present calculations, we note that the energy difference between the two lowest-lying channels obtained in this study, 21 889 cm^{-1}, is also in very good agreement with the one determined experimentally as the average of the atomic multiplets, 21 980 cm^{-1} [29].

As clearly illustrated in Fig. 1, this study extends the present limited information on the electronic states of BeBr by providing a reliable picture of the potential energy curves up to the dissociation limit and the spectroscopic parameters of not only the states X and A, but also of the states B $^2\Pi$ and C $^2\Sigma^+$ as yet not experimentally detected. These two states also show a very close resemblance to the ones investigated for the isovalent species BeCl. Close to 4.4 a_0, the A $^2\Pi$ state correlating diabatically with the second dissociation channel, and the repulsive B $^2\Pi$ correlating with the first dissociation limit show an avoided crossing which gives rise to an energy barrier for dissociation of 5149 cm^{-1}, smaller than that estimated for BeCl, 8776 cm^{-1}; its dissociation limit (without spin–orbit interactions) lies only 337 cm^{-1} below the potential energy curve minimum. In the case of BeCl, in our previous investigation, we determined the excitation energy (T_e) for the A and B states as 28 464 and 38 801 cm^{-1}, respectively; for BeBr, we found T_e values of 26 661 and 33 499 cm^{-1}. In the case of the state C $^2\Sigma^+$, an early avoided crossing at about 3.8 a_0 with a higher lying $^2\Sigma^+$ state gives rise to an energy barrier significantly smaller (630 cm^{-1}) than the one estimated for BeCl (4166 cm^{-1}), but since this state necessarily correlates with the second dissociation limit due to another avoided crossing with the ground state potential energy curve, a second minimum appears at a large internuclear distance of 5.936 a_0 (3.141 Å). This external minimum is located at 34 427 cm^{-1} (T_e) relative to the ground state, whereas for the internal one we obtained 48 374 cm^{-1} for T_e, and 3.581 a_0 (1.895 Å) for R_e.

The ground electronic state can be basically symbolized by the electronic configuration $\ldots 6\sigma^2\, 7\sigma^2\, 3\pi^4\, 8\sigma^1\, c_0^2 \sim 0.92$), close to the equilibrium distance, whereas for the A $^2\Pi$ state we can write $\ldots 6\sigma^2\, 7\sigma^2\, 3\pi^4\, 4\pi^1\, c_0^2 \sim 0.90$); the A $^2\Pi$ state can be seen as resulting from the $8\sigma \rightarrow 4\pi$ electron promotion. Using a simple molecular orbital language, the major contributions to orbitals 3π and 4π can be written as: $3\pi \approx 0.17\ (2p^{Be}) + 0.96\ (3p^{Br})$ and $4\pi \approx 0.98\ (2p^{Be}) - 0.32\ (4p^{Br})$, mostly localized on the bromine and beryllium atoms, respectively. Orbital 7σ corresponds to a bonding orbital between an *sp* hybrid of Be and the $4p_z$ of bromine, and 8σ is the other *sp* hybrid of beryllium associated with the single electron.

For the shallow curve associated with the smaller equilibrium distance we have been able to estimate only the value of the zero point energy, 364 cm^{-1}. As in the case of BeCl, this internal part of the C $^2\Sigma^+$ state is crossed by the states B $^2\Pi$ and a $^4\Sigma^+$ very close to $v' = 0$; for the external section of the potential energy curve this crossing occurs at $R \sim 4.9\ a_0$. Experimentally, electronic transitions from the C $^2\Sigma^+$ state have not as yet been observed, to the best of our knowledge.

For the sake of completeness, we list in Table 2 the vibrational levels spacings $\Delta G_{v+1/2}$ used to derive the vibrational parameters presented in Table 1; rotational constants for selected vibrational states of the low-lying electronic states are collected in Table 3. The determination of these parameters is dependent on the number of spacings and also on the number of adjusting parameters as discussed by Richards et al. [30].

For the ground state dissociation energy D_e, our first estimate is 77.31 kcal mol^{-1} (3.35 eV, 27 038 cm^{-1}); with the inclusion of the zero-point energy we obtained 76.28 kcal mol^{-1} (3.31 eV, 26 679 cm^{-1}) for D_0. If we additionally take into account the lowering in energy at the dissociation limit due to contribution of spin–

Table 1
Excitation energies (T_e, in cm^{-1}), equilibrium distances in a_0 (Å), rotational and vibrational constants (in cm^{-1}), and dissociation energies (in kcal mol^{-1}) for the BeBr molecule. Figures in parenthesis refer to the number of points used in the numerical fitting.

	T_e	R_e	B_e	ω_e	$\omega_e x_e$	D_e
X $^2\Sigma^+$	0.0	3.694 (1.955)	0.5455 (10)	715.9 (20)	3.592	77.31
Exp.	0.0	3.6911 (1.9532)[a]	0.5459[a]	715.1[b]	4.30[b]	– – –
A $^2\Pi$	26 661	3.731 (1.975)	0.5349 (7)	700.0 (6)	3.492	14.72[c]
A $^2\Pi_{1/2}$	26 551	3.728 (1.973)		696.8 (6)		17.18[c]
A $^2\Pi_{3/2}$	26 758	3.736 (1.977)		686.4 (3)		11.89[c]
Exp.	26437.6[a]	3.7351 (1.9767)[a]	0.5332[a]	702.3	3.98	– – –
B $^2\Pi$	33 449	4.485 (2.373)	0.3702 (10)	800.6 (15)	12.642	44.02
B $^2\Pi_{3/2}$	33 149	4.418 (2.338)		841.4 (4)		
B $^2\Pi_{1/2}$	33 849	4.539 (2.402)		989.5 (4)		12.34c
C $^2\Sigma^+$ (int.)	48 374	3.581 (1.895)				1.80[c]
C $^2\Sigma^+$ (ext.)	34 427	5.936 (3.141)	0.2113 (10)	313.9 (19)	1.015	
a $^4\Sigma^+$	45 644	4.416 (2.337)	0.3768 (10)	294.0 (9)	7.473	
b $^4\Delta$	46 874	4.616 (2.442)	0.3494 (7)	237.2 (6)	7.709	

[a] Experimental values of R_0, B_0, and T_{00}, Ref. [4].
[b] Vibrational constants derived from the Q_1 band head, Ref. [3].
[c] Refer to the barrier height.

Table 2
Vibrational levels spacings $\Delta G_{v+1/2}$ (in cm^{-1}) and zero-point energies (E_0) for selected electronic states of BeBr.[a]

v	X $^2\Sigma^+$	A $^2\Pi$	B $^2\Pi$	C $^2\Sigma^+$(ext.)	a $^4\Sigma^+$	a $^4\Delta$
0	710	695	864	313	280	222
1	700	685	786	311	265	206
2	693	678	725	308	249	192
3	687	671	676	306	233	175
4	680	664	638	304	219	159
5	673		609	302	204	145
6	666		585	300	189	
7	659		565	298		
8	652		547	295		
9	644		531	293		
E_0	359	353	455	166	147	118

[a] G_0 = 364 cm^{-1} for C $^2\Sigma^+$(int).

Table 3
The rotational constant B_v (in cm^{-1}) for selected vibrational states of the low-lying electronic states of BeBr.

v	X $^2\Sigma^+$	A $^2\Pi$	B $^2\Pi$	C $^2\Sigma^+$(ext.)	a $^4\Sigma^+$	b $^4\Delta$
0	0.5434	0.5323	0.3715	0.2117	0.3720	0.3435
1	0.5389	0.5277	0.3741	0.2126	0.3615	0.3313
2	0.5343	0.5232	0.3763	0.2133	0.3515	0.3196
3	0.5299	0.5187	0.3781	0.2139	0.3407	0.3068
4	0.5257	0.5142	0.3785	0.2145	0.3298	0.2933
5	0.5214	0.5099	0.3781	0.2149	0.3187	0.2799
6	0.5172		0.3772	0.2153	0.3071	0.2667
7	0.5128		0.3760	0.2156	0.2950	
8	0.5085		0.3743	0.2158	0.2827	
9	0.5041		0.3725	0.2160	0.2780	

orbit effects of the bromine atom, a better estimate of D_0 would be 72.77 kcal mol^{-1} (3.16 eV, 25 451 cm^{-1}). This latter contribution was evaluated as the weighted average over the experimental multiplets of the bromine atom, 3.51 kcal mol^{-1}. We note that this value of D_0 supports the estimate of Kleinschmidt and Hildenbrand [5] of 71 kcal mol^{-1} based on a correlation of thermochemical properties across the entire alkaline earth halide series, and definitely excludes the empirically determined value of 91.31 kcal mol^{-1} reported by Reddy et al. [6]. The expression used by these authors to estimate the bond dissociation energy (D_{AB}) assumes that it can written as the geometrical average of the bond energies of the corresponding homonuclear molecules, $(D_{AA}D_{BB})^{1/2}$, plus another term accounting for the ionic contribution to the bond using a definition of partial charge based on Pauling electronegativity differences. Since partial charges and electronegativity are not concepts directly derived from first principles of quantum mechanics, as well as the contribution of the geometrical mean to the bond energy, there is no guarantee that one can get the right answer for the right reason using this type of equation. For the set of 16 alkaline earth halide molecules investigated by Reddy et al. [6], they claim an average percentage deviation of 7.5%, but several of the experimental bond energies used were approximate values. Any close agreement is likely fortuitous. For the series BeF, BeCl, and BeBr, we have estimated their dissociation energy (D_0) as: 134.67 [20], 92.24 [8], and 72.77 kcal mol^{-1}, respectively.

Most of the other states correlating with the second dissociation channel are either repulsive or show a very shallow well. For the state a $^4\Sigma^+$ (T_e = 45 644 cm^{-1}), we estimated R_e = 4.416 a_0 (2.337 Å) and ω_e = 294 cm^{-1}, while for the state b $^4\Delta$ (T_e = 46 874 - cm^{-1}), we obtained R_e = 4.616 a_0 (2.442 Å) and ω_e = 237 cm^{-1}.

The effect of spin–orbit interactions on the $^2\Pi$ states and in regions of curve crossing of the states $^2\Pi$ with $^2\Sigma^+$ was next investigated. The resulting energy splitting is illustrated in Fig. 2 for the low-lying relativistic Ω states; the associated spectroscopic parameters characterizing these states are also collected in Table 1. One can see that for the A $^2\Pi$ state this splitting is relatively small, 207 cm^{-1} at R = 3.75 a_0, which compares quite well with the coupling constant derived experimentally, 198 cm^{-1} [4]. This result can be rationalized by noting first that at this internuclear distance this state can be associated with the electronic configuration $\ldots 7\sigma^2\ 3\pi^4\ 4\pi^1\ 8\sigma^0$, and that an analysis of the singly occupied 4π molecular orbital indicates a major contribution of beryllium $2p_z$ orbital, and thus the electron is mostly localized around the Be atom. On the other hand, the splitting of the B $^2\Pi$ state at 3.75 a_0, a distance close to the equilibrium one of the state A $^2\Pi$, we obtained a much larger splitting of 1960 cm^{-1}. Looking at the dominant electron configuration of the B $^2\Pi$ state at this distance, $\ldots 7\sigma^2\ 3\pi^3\ 8\sigma^2$, and by noting that orbital 3π is mostly localized on the bromine atom, one can easily rationalize this much larger splitting. As the internuclear distance gets larger past the avoided crossing region, the energy gap between the A $^2\Pi_{1/2}$ and A $^2\Pi_{3/2}$ states increases, but now with the Ω = 3/2 state lower in energy. At the distance of 8.0 a_0, we obtained 3446 cm^{-1}, a value in good accord with the energy difference between the multiplets Br($^2P_{3/2}$) and Br($^2P_{1/2}$), which is known experimentally to be 3685 cm^{-1}. Another interesting feature to note in Fig. 2 is that the allowed crossing shown in Fig. 1 between the states B $^2\Pi$ and C $^2\Sigma^+$ (ext) gives rise to another avoided crossing now between two Ω = 1/2 curves. Also, the state Ω = 3/2 arising from the state B $^2\Pi$ dissociates into the second channel, but the other Ω = 1/2 component avoids a crossing with the Ω = 1/2 component arising from the state C $^2\Sigma^+$ and a very perturbed potential energy curve results from this interaction. The Ω = 1/2 state with a second minimum close to R = 6.0 a_0 has the character of the former C $^2\Sigma^+$ (ext). Finally, an important point to note concerns the internal minimum of the C $^2\Sigma^+$ state. Fig. 1 shows clearly that we could locate one vibrational level for this shallow potential well. However, this state is crossed by both the B $^2\Pi$ and a $^4\Sigma^+$ states and due to the interaction among the Ω = 1/2 states, the minimum observed in the Λ + S representation disappears. A practical consequence of this interaction is that C $^2\Sigma^+$ – X $^2\Pi$ transitions are not likely to occur for BeBr in contrast to the ones observed for BeCl. In fact, such transitions have not been observed so far.

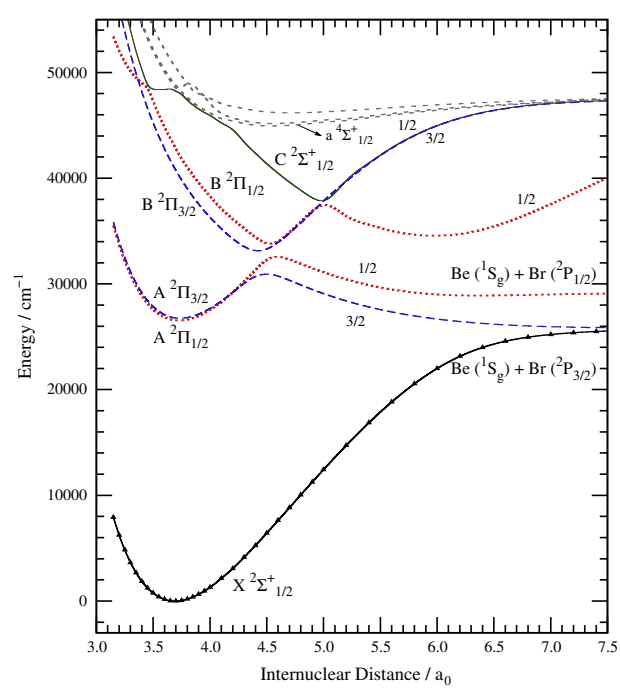

Fig. 2. Potential energy curves of the lowest-lying Ω states of the molecule BeBr.

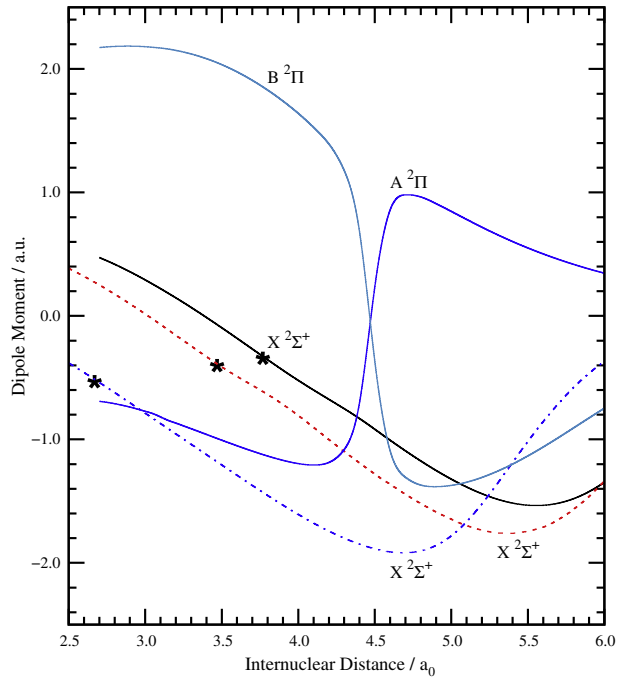

Fig. 3. Dipole moment functions of selected electronic states of the molecules: BeBr, in solid lines; BeCl, - - - - - - -; BeF, - • - • - • - • - • - • -. The symbol * indicates approximately the equilibrium distances.

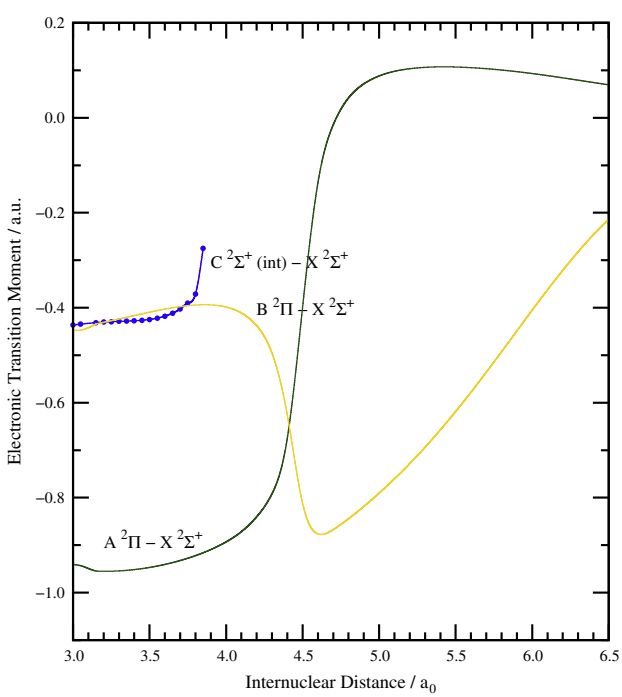

Fig. 4. Transition dipole moments of selected electronic transitions of the molecule BeBr.

3.2. Dipole and transition dipole moment functions, transition probabilities, and radiative lifetimes

The change in the molecular dipole moment as a function of the internuclear distance for selected electronic states is shown in Fig. 3. For the ground state, it is evident the linear increase in polarity ($Be^{\delta+}Br^{\delta-}$) from about −0.27 a.u. (−0.686 D) around the equilibrium distance to −1.40 a.u. (−3.557 D) close to 5.2 a_0. Since the molecule is expected to dissociate into neutral atoms, beyond about 5.5 a_0 the wavefunction necessarily changes its character to reflect the unpolarized system with zero dipole moment at large internuclear distances. In the excited state A $^2\Pi$, the molecule is more polar, as clearly reflected in the value of the dipole moment in the proximity of the equilibrium region, −1.1 a.u. (−2.785 D). However, around the region where the potential energy curves of the two $^2\Pi$ states avoid a crossing, their dipole moment functions change abruptly, with that of the A state taking the character of the B state and vice versa. In the state B $^2\Pi$ and in the vicinity of the equilibrium region of the A $^2\Pi$ state, this species has an inverted polarity ($Be^{\delta-}Br^{\delta+}$), and at large distances their dipoles also necessarily approach zero. For a more direct comparison of the molecular polarity between BeBr, BeCl, and BeF, we have also plotted in Fig. 3 the dipole moment function of BeCl obtained in our previous study [8], and values here calculated for BeF at the CASSCF/MRCI/aV5Z level of theory. From the almost parallelism of the three plots, one can conclude that the rate of change of the polarity with internuclear distance is about the same for the three species.

Concerning the transition dipole moment functions, we focused this study on the A – X, B – X, and C (int) – X systems, this latter one restricted to the region of the internal minimum of the C $^2\Sigma^+$ state; their profiles are shown in Fig. 4. For the A – X system, this function shows a slightly varying behavior up to $R \sim 4.4\ a_0$, with an average value close to −0.95 a.u.. To better analyze this behavior, we recall that in the proximity of 3.7 a_0, the electronic configurations of the states X and A can be represented by $\ldots 7\sigma^2\ 8\sigma^1\ 3\pi^4$ and $\ldots 7\sigma^2\ 8\sigma^0\ 3\pi^4\ 4\pi^1$, respectively, making evident the $8\sigma^1 \rightarrow 4\pi^1$ electron excitation, with both 8σ and 4π mostly localized on the Be atom. This result is consistent with the fact that the state A $^2\Pi$ is regular, and also with the relatively small spin–orbit

Table 4
Einstein emission $A_{v'v''}$ (s^{-1}) coefficients, Franck–Condon factors (in italics), and transition energies $T_{v'v''}$ (cm^{-1}, in parentheses) for the A $^2\Pi$ – X $^2\Sigma^+$ system of the species BeBr.

v''	v' = 0	v' = 1	v' = 2	v' = 3
0	**31 960 000** ***0.965*** (26 654)	1 333 800 0.033 (27 350)	58 261 0.001 (28 034)	3031 0.001 (28 712)
1	931 070 0.035 (25 945)	**29 358 000** ***0.898*** (26 640)	2 532 400 0.063 **(27 325)**	162 140 0.004 (28 003)
2	1345 0.000 (25 245)	1 809 100 0.068 (25 940)	**26 862 000** ***0.834*** (26 625)	3 600 100 0.090 (27 303)
3	17 0.000 (24 552)	3995 0.000 (25 247)	2 609 100 0.101 (25 932)	**24 443 000** ***0.772*** (26 610)
4	0 0.000 (23 865)	65 0.000 (24 560)	7478 0.001 (25 245)	3 343 600 0.133 (25 923)
$Q_{v'}$ [a]	1.000	1.000	1.000	1.000

[a] $Q_{v'} = \sum_{v''=0}^{5} q_{v'v''}$.

Table 5
Total Einstein $A_{v'}$ (bound–bound) coefficients and radiative lifetimes ($\tau_{v'}$, in ns) of some vibrational levels of the A $^2\Pi$ State of BeBr.

v'	A – X	$\tau_{v'}$ A
0	32 892 432	30
1	32 504 960	31
2	32 069 239	31
3	31 551 871	32

coupling constant determined experimentally and the one calculated in this work. The abrupt variation beyond this region is a consequence of the change in character of the wavefunctions due to the avoided crossing. This slightly varying function and the fact that the relative minima of the two states are very close imply that the transitions are expected to be diagonally dominant, as experimentally observed (see Fig. 4). To better quantify the A − X system, Table 4 summarizes the results of transition probabilities calculated as Einstein coefficients for emission $A_{v'v''}$, Franck–Condon factors based on this theoretical study, and transition energies $T_{v'v''}$. Clearly, relative intensities based on transition probabilities calculated as Einstein coefficients for emission and on Franck–Condon factors are in perfect agreement. Also as mentioned before, our estimate of T_{00}, 26 654 cm^{-1}, is in very good agreement with the transition energy determined by Carleer et al. 26437.6 cm^{-1} [4]. The total Einstein $A_{v'}$ coefficients for emission for selected vibrational levels of the state A $^2\Pi$ and the associated radiative lifetimes are collected in Table 5.

4. Conclusions

The low-lying electronic states of the species BeBr are characterized for the first time in the literature. Using a high-level theoretical approach, very reliable potential energy curves were constructed and the associated spectroscopic parameters determined. This study significantly expands the limited spectroscopic data on this system. The present results are contrasted with those for BeCl for which considerable experimental data exist in the literature. Account of spin–orbit interactions significantly change the $\Lambda + S$ potential energy curves, especially in regions of avoided and curve crossings involving the states A $^2\Pi$, B $^2\Pi$, and C $^2\Sigma^+$. Our estimate of spin–orbit coupling constant for the A $^2\Pi$ state is in good agreement with the value determined experimentally. The very good agreement of our results with the limited experimental data known so far guarantees the reliability of the present calculations for the states as yet experimentally unknown. For the A $^2\Pi$ − X $^2\Sigma^+$ system the transition moment function was evaluated and transition probabilities for emission computed as the Einstein $A_{v'v''}$ emission coefficients; the calculation of radiative lifetimes completed the characterization of the A $^2\Pi$ state. We expect the present results can motivate and guide future experimental studies on this system.

Acknowledgments

J.C.B. de Lima expresses his gratitute to CAPES of Brazil for a doctoral fellowship, and F.R. Ornellas acknowledges the academic support of the Conselho Nacional de Desenvolvimento Científico e Tecnológico (CNPq) of Brazil.

References

[1] Y.P. Reddy, P.T. Rao, Curr. Sci. 36 (1967) 399.
[2] Y.P. Reddy, P.T. Rao, J. Phys. B: At. Mol. Phys. 1 (1968) 482.
[3] B.R. Reddy, Y.P. Reddy, P.T. Rao, J. Phys. B: At. Mol. Phys. 3 (1970) L1.
[4] M. Carleer, M. Herman, R. Colin, Can. J. Phys. 53 (1975) 1321.
[5] P.D. Kleinschmidt, D.L. Hildenbrand, J. Chem. Phys. 68 (1978) 2819.
[6] R.R. Reddy, A.S.R. Reddy, V.K. Reddy, Can. J. Chem. 63 (1985) 3174.
[7] N.E. Kuz'menko, L.V. Chumak, J. Quant. Spectr. Radiat. Trans. 35 (1986) 419.
[8] J.C.B. de Lima, F.R. Ornellas, J. Mol. Spectr. 283 (2013) 22.
[9] G. Herzberg, Molecular Spectra and Molecular Structure. I: Spectra of Diatomic Molecules, Van Nostrand Reinhold, New York, 1950.
[10] P.J. Knowles, H.-J. Werner, J. Chem. Phys. 82 (1985) 5053.
[11] H.-J. Werner, P.J. Knowles, Chem. Phys. Lett. 115 (1985) 259.
[12] P.J. Knowles, H.-J. Werner, Chem. Phys. Lett. 82 (1988) 514.
[13] H.-J. Werner, P.J. Knowles, J. Chem. Phys. 89 (1988) 5803.
[14] H.-J. Werner, P.J. Knowles, R. Lindh, F.R. Manby, M. Schütz, and others *Molpro*, Version 2009.1, A package of Ab Initio Programs, Cardiff University, Cardiff, U.K., 2009. <http://www.molpro.net>.
[15] B. Prascher, D.E. Woon, K.A. Peterson, T.H. Dunning Jr., A.K. Wilson, Theor. Chem. Acc. 128 (2011) 69.
[16] K.A. Peterson, D. Figgen, E. Goll, H. Stoll, M. Dolg, J. Chem. Phys. 119 (2003) 11113.
[17] W.T. Zemke, W.C. Stwalley, QCPE Bull. 4 (1981) 79.
[18] E.R. Davidson, D.W. Silver, Chem. Phys. Lett. 52 (1977) 403.
[19] H.-J. Werner, M. Kállay, J. Gauss, J. Chem. Phys. 128 (2008) 034305.
[20] F.R. Ornellas, F.B.C. Machado, O. Roberto-Neto, Mol. Phys. 77 (1992) 1169.
[21] F.R. Ornellas, A.R.S. Valentim, J. Phys. Chem. 98 (1994) 12570.
[22] F.R. Ornellas, J. Chem. Phys. 125 (2006) 114314.
[23] A.C. Borin, F.R. Ornellas, Chem. Phys. 184 (1994) 59.
[24] F.R. Ornellas, W.C. Stwalley, W.T. Zemke, J. Chem. Phys. 79 (1983) 5311.
[25] F.B.C. Machado, O. Roberto-Neto, F.R. Ornellas, Chem. Phys. Lett. 284 (1998) 293.
[26] E.E. Whiting, A. Schadee, J.B. Tatum, J.T. Hougen, R.W. Nichols, J. Mol. Spectrosc. 80 (1983) 249.
[27] M. Larsson, Astron. Astrophys. 128 (1983) 291.
[28] A. Berning, M. Schweizer, H.-J. Werner, P.J. Knowles, P. Palmieri, Mol. Phys. 98 (2000) 1283.
[29] A.A. Radzig, B.M. Smirnov, Reference Data on Atoms, Molecules, and Ions, Springer-Verlag, Berlin, 1985.
[30] W.G. Richards, J. Raftery, R.K. Hinkley, in: R.N. Dixon (Ed.), Theoretical Chemistry – Quantum Chemistry, vol. I, The Chemical Society, London, 1973. Chapter 1.